Biophysical Reports, Volume *1*

Supplemental information

Diagnosing and mitigating method-based avidity artifacts that confound polyubiquitin-binding assays

Allyn J. Schoeffler, Elizabeth Helgason, Nataliya Popovych, and Erin C. Dueber

Supplemental Materials

Diagnosing and mitigating method-based avidity artifacts that confound polyubiquitin binding assays

Allyn J. Schoeffler[1,2], Elizabeth Helgason[1], Nataliya Popovych[1], Erin C. Dueber[1*]

[1]Department of Early Discovery Biochemistry, Genentech, 1 DNA Way, South San Francisco, CA 94080

[2]Present address: Department of Chemistry and Biochemistry, Loyola University, New Orleans, 6363 St. Charles Ave New Orleans, LA 70118

*Correspondence: dueber.erin@gene.com

Fig. S1

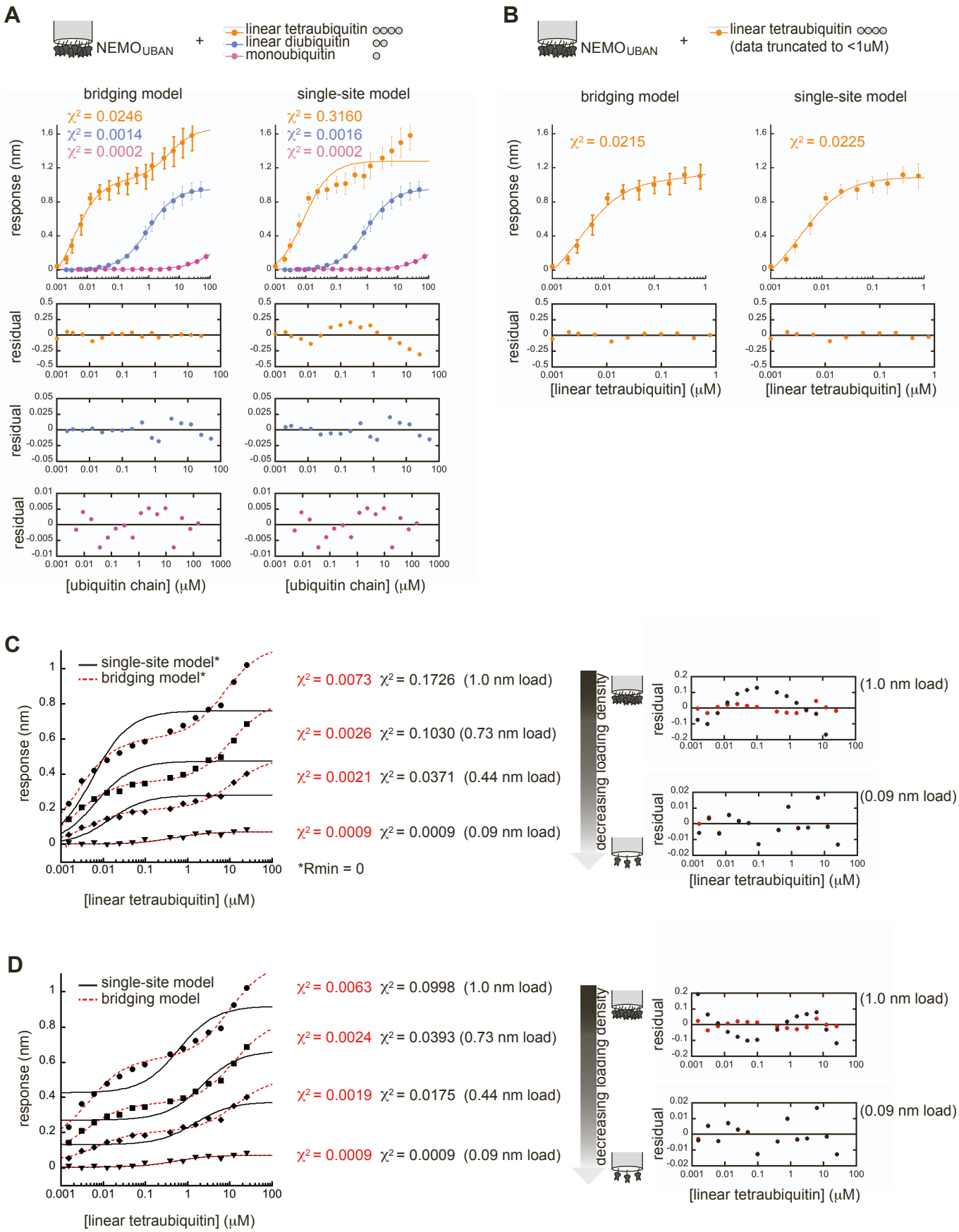
A
NEMO$_{UBAN}$
+
linear tetraubiquitin
linear diubiquitin
monoubiquitin
bridging model
single-site model
χ^2 = 0.0246
χ^2 = 0.0014
χ^2 = 0.0002
χ^2 = 0.3160
χ^2 = 0.0016
χ^2 = 0.0002
response (nm)
residual
residual
residual
[ubiquitin chain] (μM)
[ubiquitin chain] (μM)
B
NEMO$_{UBAN}$
+
linear tetraubiquitin
(data truncated to <1uM)
bridging model
single-site model
χ^2 = 0.0215
χ^2 = 0.0225
response (nm)
residual
residual
[linear tetraubiquitin] (μM)
[linear tetraubiquitin] (μM)
C
single-site model*
bridging model*
response (nm)
[linear tetraubiquitin] (μM)
χ^2 = 0.0073 χ^2 = 0.1726 (1.0 nm load)
χ^2 = 0.0026 χ^2 = 0.1030 (0.73 nm load)
χ^2 = 0.0021 χ^2 = 0.0371 (0.44 nm load)
χ^2 = 0.0009 χ^2 = 0.0009 (0.09 nm load)
*Rmin = 0
decreasing loading density
residual
(1.0 nm load)
residual
(0.09 nm load)
[linear tetraubiquitin] (μM)
D
single-site model
bridging model
response (nm)
[linear tetraubiquitin] (μM)
χ^2 = 0.0063 χ^2 = 0.0998 (1.0 nm load)
χ^2 = 0.0024 χ^2 = 0.0393 (0.73 nm load)
χ^2 = 0.0019 χ^2 = 0.0175 (0.44 nm load)
χ^2 = 0.0009 χ^2 = 0.0009 (0.09 nm load)
decreasing loading density
residual
(1.0 nm load)
residual
(0.09 nm load)
[linear tetraubiquitin] (μM)

Fig. S2

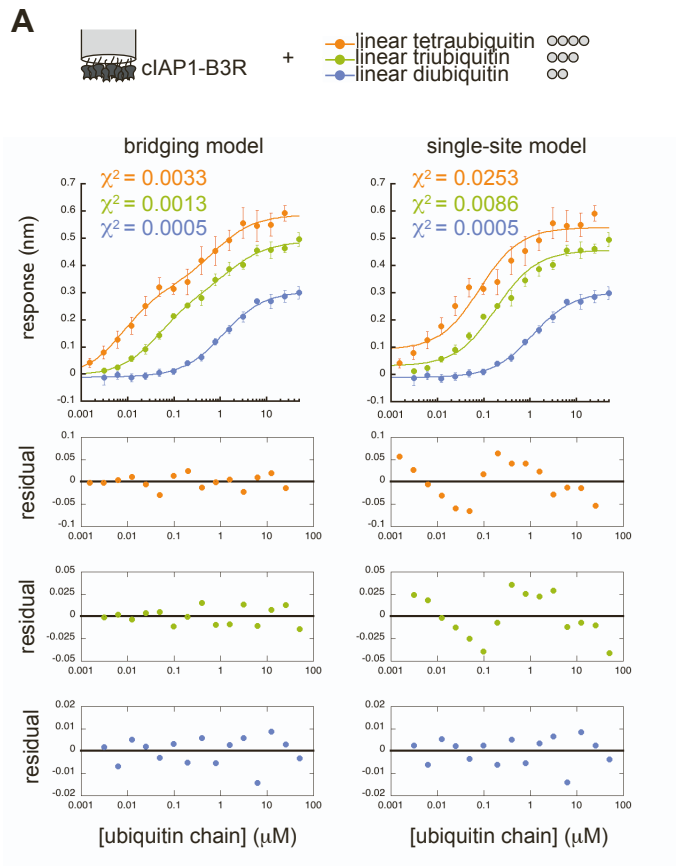
A
cIAP1-B3R
+
linear tetraubiquitin
linear triubiquitin
linear diubiquitin
bridging model
single-site model
response (nm)
residual
[ubiquitin chain] (μM)

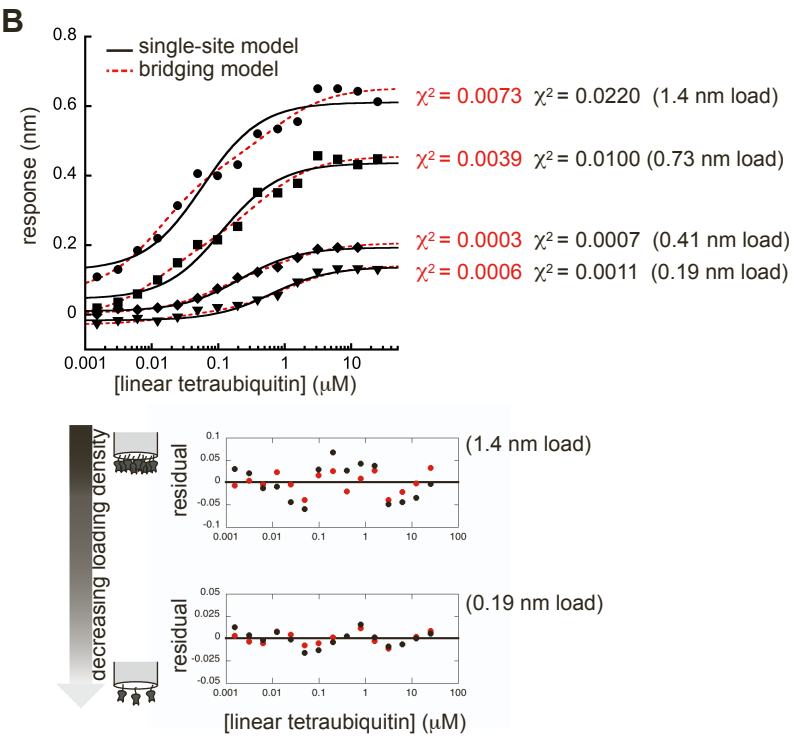
B
single-site model
bridging model
response (nm)
[linear tetraubiquitin] (μM)
(1.4 nm load)
(0.73 nm load)
(0.41 nm load)
(0.19 nm load)
decreasing loading density
residual

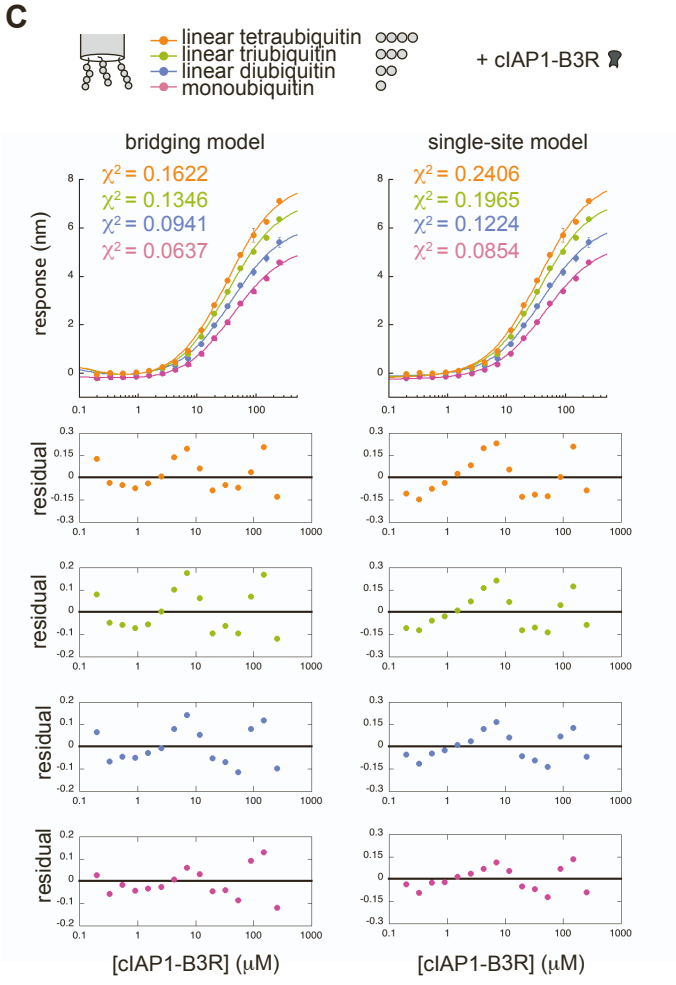
C
linear tetraubiquitin
linear triubiquitin
linear diubiquitin
monoubiquitin
+ cIAP1-B3R
bridging model
single-site model
response (nm)
residual
[cIAP1-B3R] (μM)

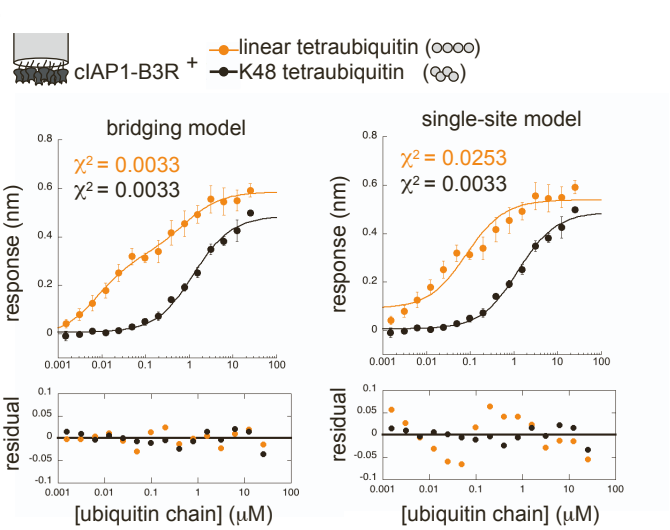
D
cIAP1-B3R
+
linear tetraubiquitin
K48 tetraubiquitin
bridging model
single-site model
response (nm)
residual
[ubiquitin chain] (μM)

Fig. S3

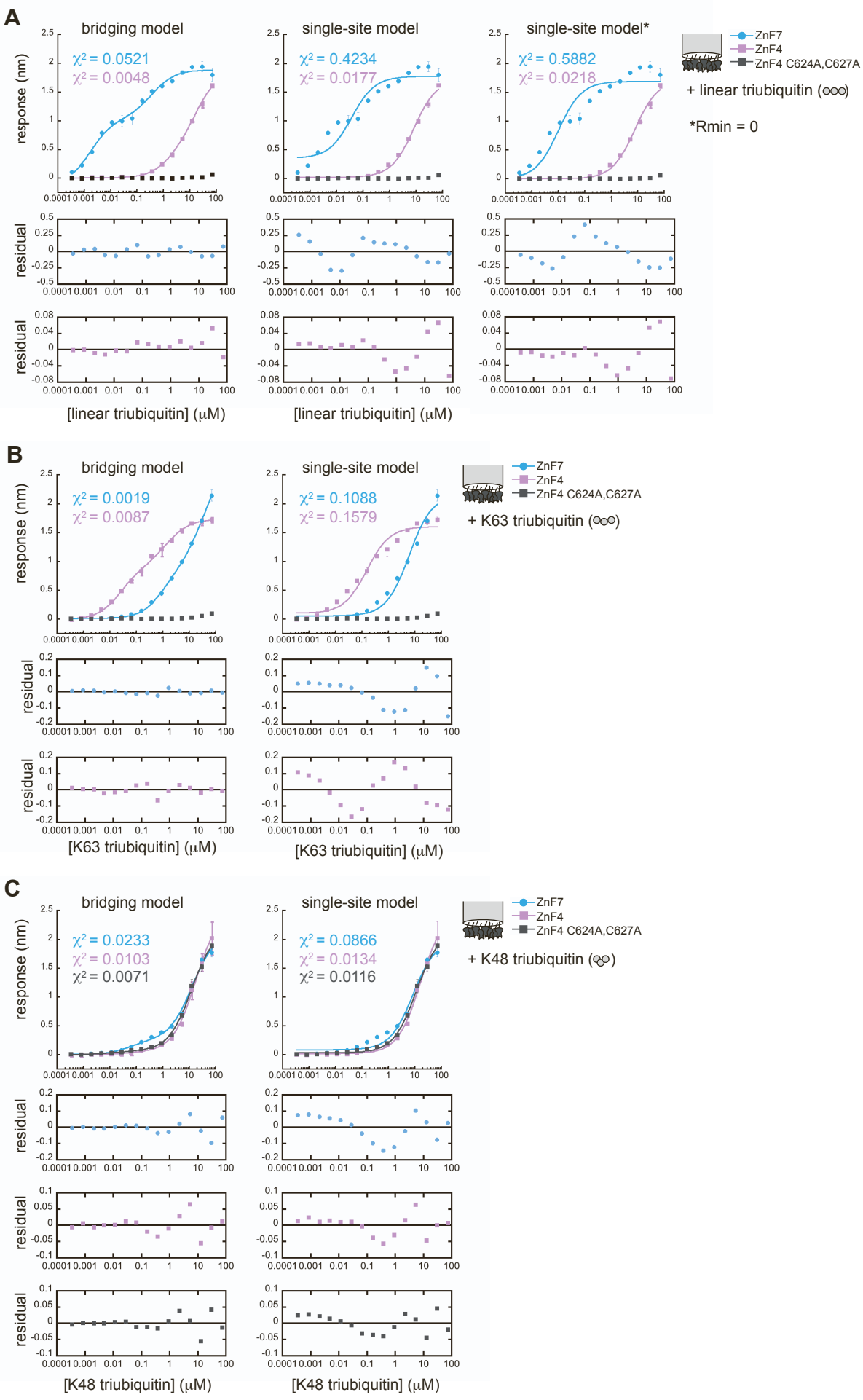
A
bridging model
single-site model
single-site model*
response (nm)
χ² = 0.0521
χ² = 0.0048
χ² = 0.4234
χ² = 0.0177
χ² = 0.5882
χ² = 0.0218
residual
[linear triubiquitin] (μM)
ZnF7
ZnF4
ZnF4 C624A,C627A
+ linear triubiquitin (∞∞)
*Rmin = 0
B
bridging model
single-site model
χ² = 0.0019
χ² = 0.0087
χ² = 0.1088
χ² = 0.1579
[K63 triubiquitin] (μM)
+ K63 triubiquitin (∞∞)
C
bridging model
single-site model
χ² = 0.0233
χ² = 0.0103
χ² = 0.0071
χ² = 0.0866
χ² = 0.0134
χ² = 0.0116
[K48 triubiquitin] (μM)
+ K48 triubiquitin (∞)

Fig. S4

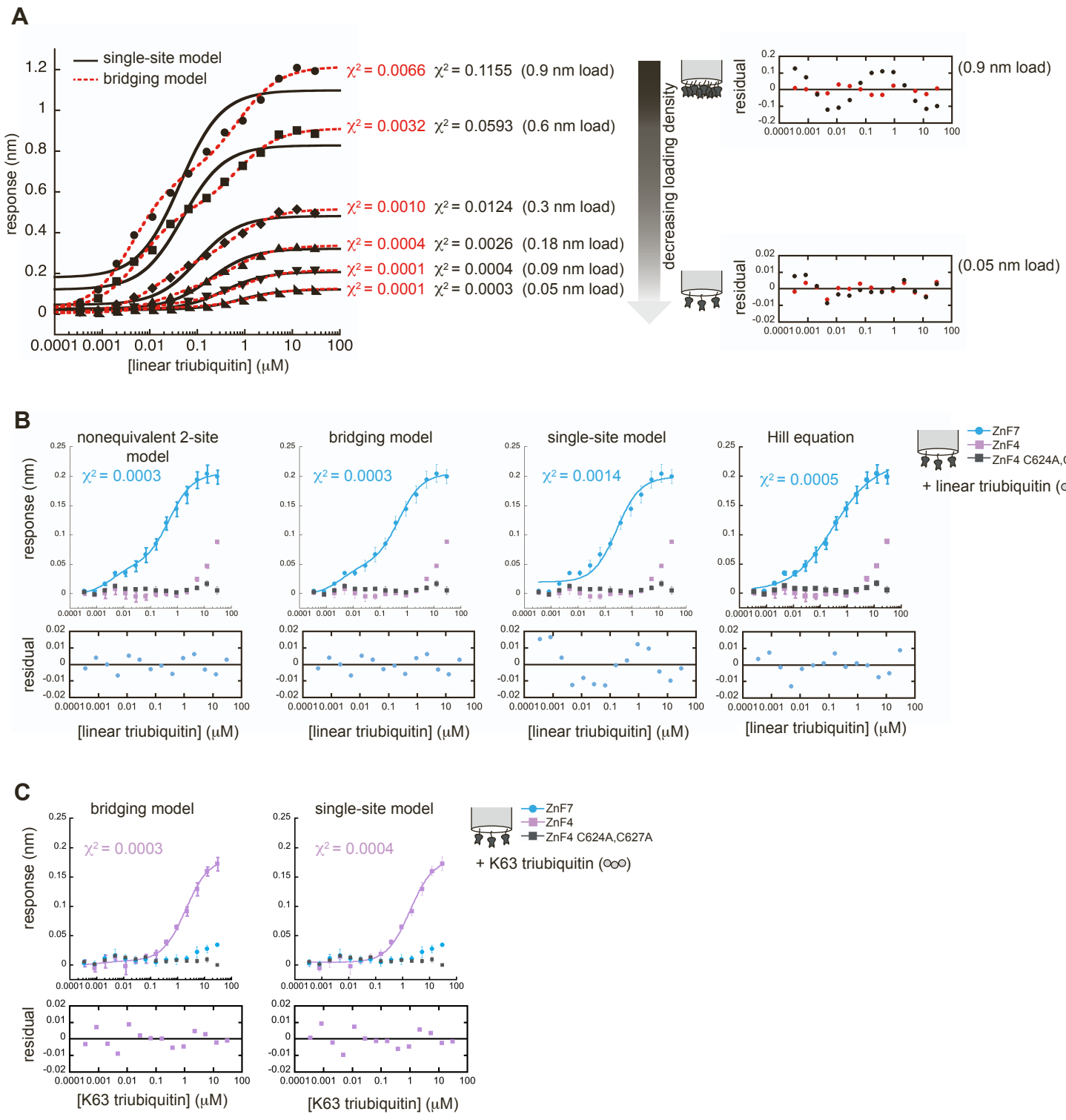
A
single-site model
bridging model
response (nm)
[linear triubiquitin] (μM)
χ² = 0.0066 χ² = 0.1155 (0.9 nm load)
χ² = 0.0032 χ² = 0.0593 (0.6 nm load)
χ² = 0.0010 χ² = 0.0124 (0.3 nm load)
χ² = 0.0004 χ² = 0.0026 (0.18 nm load)
χ² = 0.0001 χ² = 0.0004 (0.09 nm load)
χ² = 0.0001 χ² = 0.0003 (0.05 nm load)
decreasing loading density
residual
(0.9 nm load)
(0.05 nm load)
B
nonequivalent 2-site model
bridging model
single-site model
Hill equation
χ² = 0.0003
χ² = 0.0003
χ² = 0.0014
χ² = 0.0005
response (nm)
residual
[linear triubiquitin] (μM)
ZnF7
ZnF4
ZnF4 C624A,C627A
+ linear triubiquitin (∞∞)
C
bridging model
single-site model
χ² = 0.0003
χ² = 0.0004
response (nm)
residual
[K63 triubiquitin] (μM)
ZnF7
ZnF4
ZnF4 C624A,C627A
+ K63 triubiquitin (∞∞)

Fig. S5

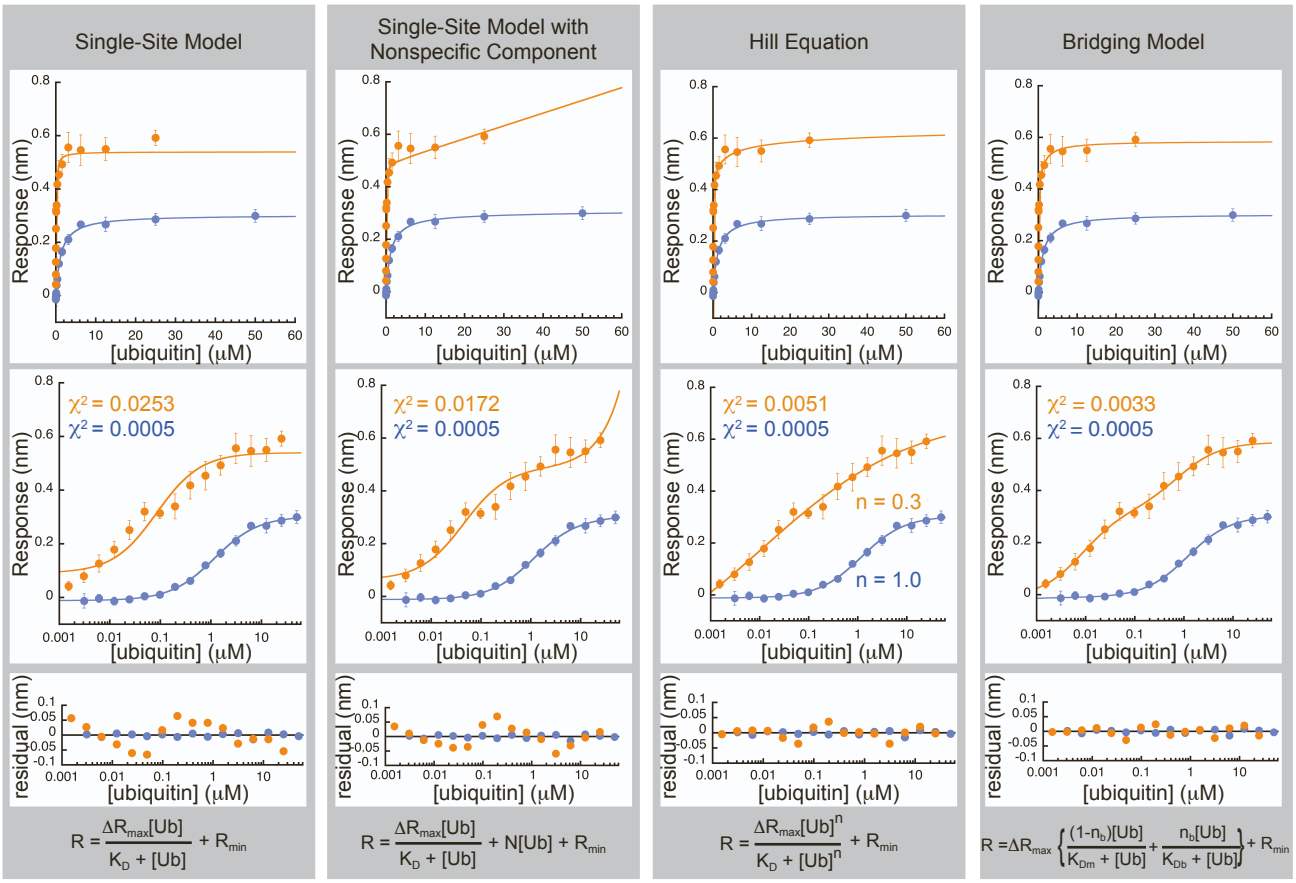
Single-Site Model
Single-Site Model with Nonspecific Component
Hill Equation
Bridging Model
Response (nm)
[ubiquitin] (μM)
residual (nm)
χ² = 0.0253
χ² = 0.0005
χ² = 0.0172
χ² = 0.0005
χ² = 0.0051
χ² = 0.0005
n = 0.3
n = 1.0
χ² = 0.0033
χ² = 0.0005
R = ΔRmax[Ub] / (KD + [Ub]) + Rmin
R = ΔRmax[Ub] / (KD + [Ub]) + N[Ub] + Rmin
R = ΔRmax[Ub]^n / (KD + [Ub]^n) + Rmin
R = ΔRmax {(1-nb)[Ub] / (KDm + [Ub]) + nb[Ub] / (KDb + [Ub])} + Rmin

Fig. S6

A

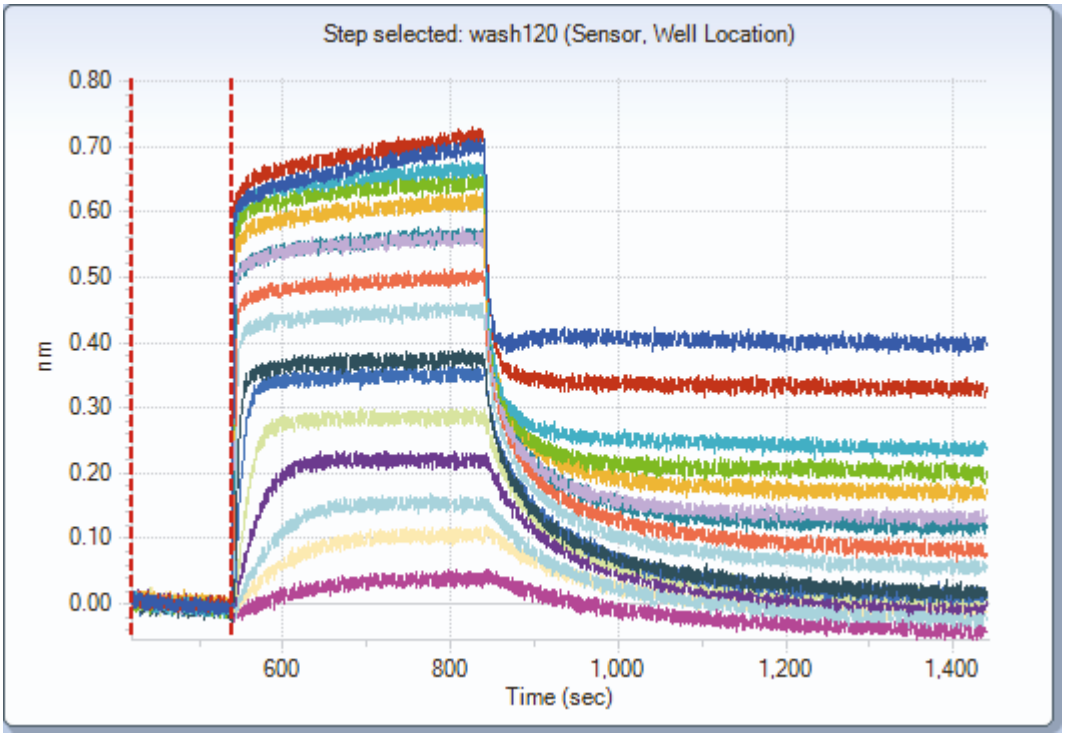

cIAP1-B3R

\+ linear tetraubiquitin (∞∞∞)

B

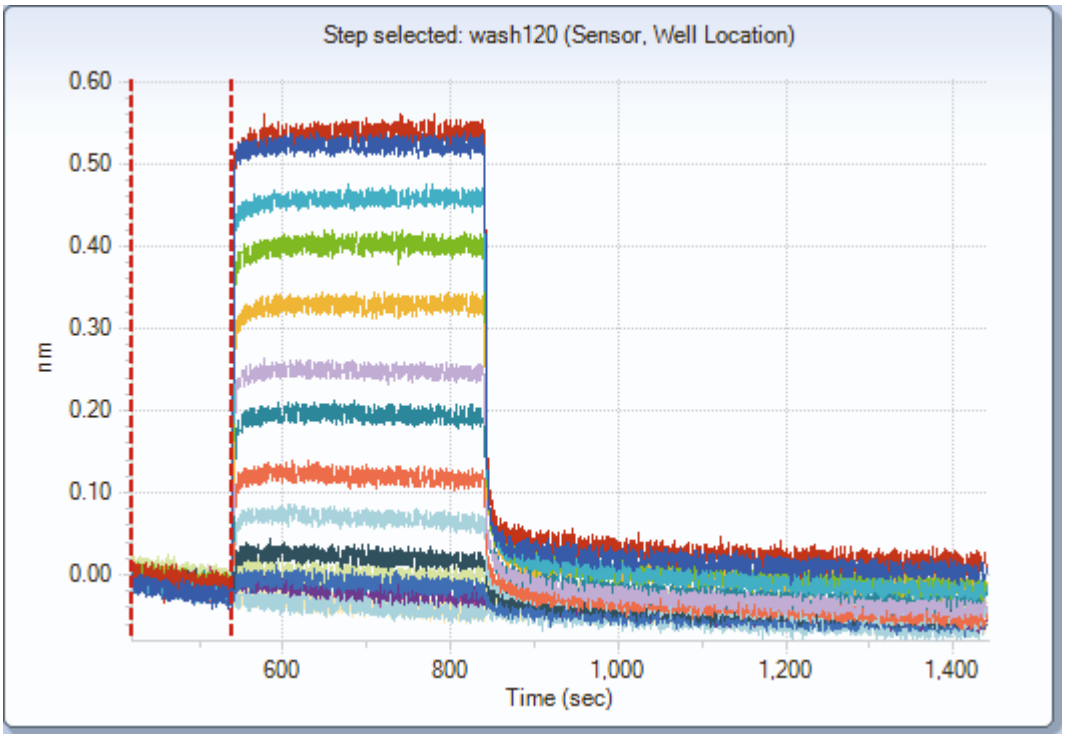

cIAP1-B3R

\+ K48 tetraubiquitin (∞)

Supplemental Figure Legends

Figure S1 Comprehensive analysis of ubiquitin binding by NEMO. (**A**) BLI measurements of monoubiquitin and linear di- and triubiquitin binding to monobiotinylated $NEMO_{UBAN}$. Curves represent fits of the bridging model (left panel) or single-site binding model (right panel) to equilibrium response data. Error bars indicate the standard deviation of three experiments. Fitting residuals, colored as in the fits, are shown below each plot. (**B**) BLI measurements of linear tetraubiquitin binding to monobiotinylated $NEMO_{UBAN}$, as in **a**, but truncated at the intermediate plateau (< 1 μM tetraubiquitin). The data are fit to a single-site model and to the bridging model, and residuals are shown below the plot. (**C**) BLI measurements of linear tetraubiquitin binding to monobiotinylated $NEMO_{UBAN}$. Curves represent fits of the bridging model or single-site binding model to equilibrium response data. In this case, the value for R_{min} has been set to zero. χ^2 values for both fitting models and measured loading densities are reported to the right of the plot, followed by fitting residuals for the highest and lowest loading density data. (**D**) The data from **b** are reproduced here, but fit to the bridging model in which R_{min} is a fittable parameter. All fitting parameters from these fits may be found in **Table S1**.

Figure S2 Comprehensive analysis of ubiquitin binding by cIAP1. (**A**) BLI measurements of linear di-, tri- and tetraubiquitin binding to monobiotinylated cIAP1-B3R. Curves represent fits of the bridging model (left panel) or single-site binding model (right panel) to equilibrium response data. Error bars indicate the standard deviation of three experiments. Fitting residuals, colored as in the fits, are shown below each plot. (**B**) BLI measurements of linear tetraubiquitin binding to monobiotinylated cIAP1-B3R. Curves represent fits of the

bridging model or single-site binding model to equilibrium response data. χ^2 values for both fitting models and measured loading densities are reported to the right of the plot. Fitting residuals for the highest and lowest loading density data are shown in the lower panel. (**C**) BLI measurements of cIAP1-B3R binding to monobiotinylated monoubiquitin or linear di-, tri- and tetraubiquitin. Curves represent fits of the bridging model (left panel) or single-site binding model (right panel) to equilibrium response data. Error bars indicate the standard deviation of three experiments. Fitting residuals, colored as in the fits, are shown below each plot. χ^2 values are shown inset. (**D**) BLI measurements of linear and K48-linked tetraubiquitin binding to monobiotinylated cIAP1-B3R. Curves represent fits of the bridging model (left panel) or single-site binding model (right panel) to equilibrium response data. Error bars indicate the standard deviation of three experiments. Fitting residuals, colored as in the fits, are shown below each plot. χ^2 values are shown inset. All fitting parameters from these fits may be found in **Table S1**.

Figure S3 Comprehensive analysis of ubiquitin binding by A20 zinc fingers, part 1. (**A**) BLI measurements of linear triubiquitin binding to monobiotinylated ZnF7, ZnF4, and ZnF4 with the C624A/C627A binding mutation at ~1 nm loading response. Curves represent fits of the bridging model (left panel) the single-site binding model (middle panel) and the single-site binding model with R_{min} set to zero (right panel) to equilibrium response data. Error bars indicate the standard deviation of three experiments. Fitting residuals, colored as in the fits, are shown below each plot. χ^2 values are shown inset. (**B**) BLI measurements, as in **a**, of K63-linked triubiquitin binding to monobiotinylated ZnF7 (blue), ZnF4 (purple), and ZnF4 with the C624A/C627A binding mutation (gray). (**C**) BLI measurements, as in **a**,

of K48-linked triubiquitin binding to monobiotinylated ZnF7 (blue), ZnF4 (purple), and ZnF4 with the C624A/C627A binding mutation (gray). All fitting parameters from these fits may be found in **Table S1**.

Figure S4. Comprehensive analysis of ubiquitin binding by A20 zinc fingers, part 2. (**A**) BLI measurements of linear triubiquitin binding to monobiotinylated ZnF7. Curves represent fits of the bridging model (dashed red line) or single-site binding model (solid black line) to equilibrium response data. χ^2 values for both fitting models and measured loading densities are reported to the right of the plot, followed by fitting residuals for the highest and lowest loading density data. (**B**) BLI measurements of linear triubiquitin binding to monobiotinylated ZnF7 (blue), ZnF4 (purple), and ZnF4 with the C624A/C627A binding mutation (gray) at ~0.1 nm loading response. Only the ZnF7 data supported nonlinear fitting. Curves represent fits of the nonequivalent two-site binding model (far left panel) the bridging model (middle left panel), the single-site binding model (middle right panel) and the Hill equation (far right panel) to equilibrium response data. Note that the nonequivalent two-site binding model fits a separate ΔR_{max} to each binding phase, as we cannot assume equal response sizes in BLI data. Error bars indicate the standard deviation of three experiments. Fitting residuals are shown below each plot; χ^2 values are shown inset. (**C**) BLI measurements of K63-linked triubiquitin binding to monobiotinylated ZnF7, ZnF4, and ZnF4 with the C624A/C627A binding mutation. Only the ZnF4 data supported nonlinear fitting. Curves represent fits of the bridging model (left panel) and the single-site binding model (right panel) to equilibrium response data. Error bars indicate the standard

deviation of three experiments. Fitting residuals are shown below each plot; χ^2 values are shown inset. All fitting parameters from these fits may be found in **Table S1**.

Figure S5. Assessing binding models with example BLI data. BLI measurements of diubiquitin (blue) and tetraubiquitin (orange) binding to monobiotinylated cIAP1-B3R. Curves through the points represent the fit of the following models to the data. First column: single site binding model; second column: single site binding model with a linear non-specific binding component; third column: cooperative model (Hill equation); fourth column: bridging model presented here. Equations are shown below the fits. In all cases, the data are fit using a signal offset (R_{min}) to account for the slight background signal in the absence of analyte, but this term may be removed if data are blanked. The top row shows the data with linear x-axes; the middle row displays the same data and fits with logarithmic x-axes. The bottom row shows residuals from the nonlinear fits. χ^2 values and n (for the Hill equation) are indicated in the middle row. Error bars indicate the standard deviation of three experiments. Note that the fit to the cooperative model returns a Hill coefficient of less than 1, indicating negative cooperativity. While the fit is reasonable, in this system, bridging is a more plausible explanation for the data than negative cooperativity. Note also that fits to linear diubiquitin data are uniformly good across all models, essentially collapsing to a single-site binding model, while fits to the tetraubiquitin data are best with the bridging model.

Figure S6. Example raw sensograms showing association and dissociation phases of BLI response. Monobiotinylated cIAP1-B3R was affixed to streptavidin BLI tips at a standard

~1 nm loading density. Tips were washed to remove unbound protein and the immersed in wells with varying concentrations of either linear tetraubiquitin (**A**) or K48-linked tetraubiquitin (**B**). Data have been normalized to the post-loading wash step. Note that in the case of linear tetraubiquitin, in which bridging artifacts are apparent in the equilibrium binding data, the dissociation phase fails to return to the baseline. In contrast, the data for the more compact K48-linked tetraubquitin, which we show here displays negligible bridging artifacts in the equilibrium response data, dissociation phases return to near baseline even at the highest ubiquitin concentrations.

Table S1 Fit parameters for bridging and single-site models

			bridging model [a]						single site model [a]			
	immobilized protein	analyte	fraction bridging	KDb, μM (bridging)	KDm, μM (monovalent)	ΔRmax	Rmin	χ2	KD, μM	ΔRmax	Rmin	χ2
Fig. 2 *B*	NEMOUBAN	linear Ub4	0.69 ± 0.03	0.004 ± 0.001	4 ± 2	1.98 ± 0.12	-0.31 ± 0.11	0.0246	0.009 ± 0.004	1.36 ± 0.17	-0.077 ± 0.18	0.3160
	NEMOUBAN	linear Ub4 (data to < 1μM)	0.57 ± 41	0.004 ± 0.001	18 ± 3000	2.4 ± 170	-0.30 ± 0.14	0.0215	0.004 ± 0.001	1.38 ± 0.10	-0.29 ± 0.11	0.0225
	NEMOUBAN	linear Ub2	0.02 ± 0.02	0.01 ± 0.05	1.0 ± 0.1	0.96 ± 0.02	-0.004 ± 0.018	0.0014	0.97 ± 0.03	0.94 ± 0.01	0.005 ±0.005	0.0016
	NEMOUBAN	Ub	0.52 ± 1e4	-5e-6 ± 0.2	101 ± 14	0.73 ± 2e4	-0.37 ± 2e4	0.0002	102 ± 12	0.35 ± 0.02	0.006 ± 0.001	0.0002
Fig. 2 *C*	NEMOUBAN 1nm load	linear Ub4	0.47 ± 0.05 *(0.53 ± 0.03)*	0.005 ± 0.002 *(0.0025 ± 0.0003)*	10 ± 4 *(8 ± 3)*	1.03 ± 0.09 *(1.13 ± 0.06)*	0.13 ± 0.07 *(set to 0)*	0.0063 *(0.0073)*	0.6 ± 0.4 *(0.006 ± 0.002)*	0.49 ± 0.07 *(0.76 ± 0.04)*	0.43 ± 0.04 *(set to 0)*	0.0098 *(0.1726)*
	NEMOUBAN 0.73 nm load	linear Ub4	0.38 ± 0.05 *(0.44 ± 0.03)*	0.004 ± 0.002 *(0.0024 ± 0.0003)*	13 ± 4 *(11 ± 3)*	0.77 ± 0.07 *(0.82 ± 0.05)*	0.07 ± 0.05 *(set to 0)*	0.0024 *(0.0026)*	2.2 ± 1.3 *(0.007 ± 0.003)*	0.39 ± 0.06 *(0.47 ± 0.03)*	0.27 ± 0.02 *(set to 0)*	0.0393 *(0.1030)*
	NEMOUBAN 0.44 nm load	linear Ub4	0.36 ± 0.06 *(0.41 ± 0.04)*	0.007 ± 0.003 *(0.004 ± 0.001)*	14 ± 7 *(12 ± 5)*	0.48 ± 0.06 *(0.49 ± 0.05)*	0.03 ± 0.03 *(set to 0)*	0.0019 *(0.0021)*	1.5 ± 0.9 *(0.01 ± 0.01)*	0.24 ± 0.04 *(0.28 ± 0.02)*	0.13 ± 0.02 *(set to 0)*	0.0175 *(0.0371)*
	NEMOUBAN 0.09 nm load	linear Ub4	-0.31 ± 160 *(0.004 ± 0.05)*	0.0001 ± 0.06 *(-0.001 ± 0.001)*	0.5 ± 0.3 *(0.5 ± 0.2)*	0.05 ± 6 *(0.07 ± 0.01)*	0.02 ± 6 *(set to 0)*	0.0009 *(0.0009)*	0.5 ± 0.2 *(0.5 ± 0.2)*	0.069 ± 0.006 *(0.07 ± 0.01)*	0.002 ± 0.004 *(set to 0)*	0.0009 *(0.0009)*
Fig. 3 *A*	CIAP1-B3R	linear Ub4	0.56 ± 0.04	0.03 ± 0.01[b]	3 ± 1[b]	0.60 ± 0.03	-0.01 ± 0.03	0.0033	0.3 ± 0.1[b]	0.45 ± 0.03	0.09 ± 0.03	0.0253
	CIAP1-B3R	linear Ub3	0.60 ± 0.06	0.15 ± 0.04[b]	5 ± 2[b]	0.49 ± 0.01	-0.01 ± 0.01	0.0013	0.6 ± 0.1[b]	0.43 ± 0.02	0.03 ± 0.02	0.0086
	CIAP1-B3R	linear Ub2	0.02 ± 0.29	0.3 ± 5[b]	2 ± 1[b]	0.32 ± 0.01	-0.01 ± 0.01	0.0005	2.3 ± 0.2[b]	0.314 ± 0.005	-0.011 ± 0.003	0.0005
Fig. 3 *B*	CIAP1-B3R 1.4 nm load	linear Ub4	0.63 ± 0.08	0.05 ± 0.03[b]	3 ± 2[b]	0.59 ± 0.04	0.07 ± 0.04	0.0073	0.2 ± 0.1[b]	0.48 ± 0.03	0.13 ± 0.03	0.0220
	CIAP1-B3R 0.73 nm load	linear Ub4	0.46 ± 0.11	0.05 ± 0.04[b]	2 ± 1[b]	0.46 ± 0.03	-0.01 ± 0.03	0.0039	0.5 ± 0.1[b]	0.39 ± 0.02	0.04 ± 0.02	0.0100
	CIAP1-B3R 0.41 nm load	linear Ub4	0.62 ± 0.19	0.4 ± 0.2[b]	5 ± 5[b]	0.20 ± 0.01	0.005 ± 0.004	0.0003	0.8 ± 0.1[b]	0.18 ± 0.01	0.010 ± 0.004	0.0007
	CIAP1-B3R 0.19 nm load	linear Ub4	0.20 ± 0.08	0.1 ± 0.1[b]	4 ± 1[b]	0.17 ± 0.01	-0.03 ± 0.01	0.0006	2.5 ± 0.5[b]	0.15 ± 0.01	-0.017 ± 0.004	0.0011
Fig. 3 *E*	linear Ub4	CIAP1-B3R	-0.2 ± 0.5	0.1 ± 0.5	32 ± 3	7.16 ± 3.20	0.79 ± 3	0.1622	36 ± 3	8.26 ± 0.16	-0.19 ± 0.06	0.2406
	linear Ub3	CIAP1-B3R	-0.3 ± 2	0.1 ± 0.4	35 ± 3	5.95 ± 10	1.24 ± 10	0.1346	38 ± 3	7.44 ± 0.15	-0.15 ± 0.06	0.1965
	linear Ub2	CIAP1-B3R	-0.3 ± 5	0.03 ± 0.5	39 ± 3	4.98 ± 19	1.20 ± 19	0.0941	41 ± 3	6.38 ± 0.13	-0.13 ± 0.04	0.1224
	Ub	CIAP1-B3R	-0.05 ± 0.03	1 ± 2	42 ± 5	5.43 ± 0.19	-0.14 ± 0.18	0.0637	47 ± 3	5.65 ± 0.11	-0.25 ± 0.04	0.0854
Fig. 3 *F*	CIAP1-B3R	linear Ub4	0.56 ± 0.04	0.03 ± 0.01[b]	3 ± 1[a]	0.60 ± 0.03	-0.01 ± 0.03	0.0033	0.3 ± 0.1[b]	0.45 ± 0.03	0.09 ± 0.03	0.0253
	CIAP1-B3R	K48 Ub4	0.9 ± 2e11	5 ± 2e7[b]	5 ± 2e8[a]	0.48 ± 0.02	0.01 ± 0.01	0.0033	5 ± 1[b]	0.48 ± 0.01	0.01 ± 0.01	0.0033
Fig. 4 *A*	ZnF4	linear Ub3	0.26 ± 0.12	2 ± 1	18 ± 6	1.89 ± 0.07	0.01 ± 0.01	0.0048	9 ± 1 *(8 ± 1)*	1.72 ± 0.05 *(1.72 ± 0.05)*	0.02 ± 0.01 *(set to 0)*	0.0177 *(0.0218)*
	ZnF4	K63 Ub3	0.53 ± 0.03	0.026 ± 0.005	1.5 ± 0.3	1.73 ± 0.03	-0.001 ± 0.02	0.0087	0.16 ± 0.04	1.50 ± 0.07	0.10 ± 0.05	0.1579
	ZnF4	K48 Ub3	0.02 ± 0.01	0.04 ± 0.09	18 ± 2	2.53 ± 0.07	-0.002 ± 0.02	0.0103	17 ± 1	2.48 ± 0.06	0.02 ± 0.01	0.0134
	ZnF7	linear Ub3	0.58 ± 0.04	0.002 ± 0.001	0.4 ± 0.1	2.00 ± 0.14	-0.11 ± 0.13	0.0521	0.04 ± 0.02 *(0.010 ± 0.003)*	1.42 ± 0.12 *(1.69 ± 0.08)*	0.35 ± 0.11 *(set to 0)*	0.4234 *(0.5882)*
	ZnF7	K63 Ub3	0.32 ± 0.01	1.1 ± 0.1	40 ± 6	2.82 ± 0.09	0.01 ± 0.01	0.0019	6 ± 1	2.10 ± 0.10	0.06 ± 0.03	0.1088
	ZnF7	K48 Ub3	0.12 ± 0.02	0.06 ± 0.05	13 ± 2	2.11 ± 0.09	0.01 ± 0.03	0.0233	9 ± 2	1.92 ± 0.11	0.09 ± 0.03	0.0866
	ZnF4 C624A/C627A	K48 Ub3	0.03 ± 0.01	0.01 ± 0.02	12 ± 1	2.19 ± 0.05	0.004 ± 0.02	0.0071	12 ± 1	2.13 ± 0.05	0.03 ± 0.01	0.0116
Fig. 4 *B*	ZnF7 1.0 nm load	linear Ub4	0.57 ± 0.02	0.005 ± 0.001	0.8 ± 0. 2	1.19 ± 0.03	0.02 ± 0.03	0.0066	0.04 ± 0.02	0.92 ± 0.07	0.18 ± 0.06	0.1155
	ZnF7 0.9 nm load	linear Ub4	0.56 ± 0.03	0.006 ± 0.001	0.7 ± 0.2	0.89 ± 0.02	0.02 ± 0.02	0.0032	0.05 ± 0.02	0.71 ± 0.05	0.12 ± 0.04	0.0593
	ZnF7 0.6 nm load	linear Ub4	0.48 ± 0.04	0.013 ± 0.003	0.6 ± 0.2	0.51 ± 0.01	0.01 ± 0.01	0.0010	0.10 ± 0.03	0.44 ± 0.02	0.05 ± 0.02	0.0124
	ZnF7 0.3 nm load	linear Ub4	0.34 ± 0.05	0.02 ± 0.01	1.1 ± 0.3	0.26 ± 0.01	0.005 ± 0.004	0.0004	0.3 ± 0.1	0.22 ± 0.01	0.02 ± 0.01	0.0026
	ZnF7 0.18 nm load	linear Ub4	0.20 ± 0.03	0.005 ± 0.004	1.3 ± 0.2	0.115 ± 0.004	0.011 ± 0.003	0.0001	0.8 ± 0.2	0.101 ± 0.005	0.021 ± 0.002	0.0004
	ZnF7 0.09 nm load	linear Ub4	0.24 ± 0.10	0.001 ± 0.001	1.3 ± 0.3	0.09 ± 0.01	-0.001 ± 0.01	0.0001	1.0 ± 0.3	0.070 ± 0.004	0.014 ± 0.002	0.0003
Fig. 4 *D*	ZnF4	linear Ub3	0.07 ± 2	-6e-5 ± 0.002	47 ± 24	0.25 ± 0.61	-0.02 ± 0.62	0.0002	51 ± 24	0.24 ± 0.08	-0.001 ± 0.001	0.0002
	ZnF4	K63 Ub3	0.09 ± 0.13	0.001 ± 0.006	2.1 ± 0.3	0.09 ± 0.01	-0.001 ± 0.01	0.0003	2.0 ± 0.2	0.18 ± 0.01	0.005 ± 0.002	0.0004
	ZnF7	linear Ub3	0.25 ± 0.03	0.003 ± 0.002	0.5 ± 0.1	0.21 ± 0.01	-0.002 ± 0.007	0.0003	0.3 ± 0.1	0.18 ± 0.01	0.020 ± 0.005	0.0014

[a] Values that are italicized and in parenthesis are fitted parameters when R_{min} is set to 0

[b] Affinity measurements are normalized to reflect the number of ubiquitin sites in solution for the 1:1 stoichiometry of the CIAP1-B3R:monoubiquitin interaction (i.e. 4x for Ub4, 3x for Ub3 and 2x for Ub2)

Table S2 Fit parameters for nonequivalent 2-site binding and cooperative binding models

		nonequivalent 2-site binding model						cooperative binding model (Hill equation)				
immobilized protein	analyte	ΔRmax (site 1)	KD1, μM (site1)	ΔRmax (site 2)	KD1, μM (site2)	Rmin	χ2	ΔRmax	KD, μM	n (Hill coefficient)	Rmin	χ2
ZnF7	linear Ub3	0.16 ± 0.01	0.5 ± 0.1	0.05 ± 0.01	0.003 ± 0.002	-0.002 ± 0.007	0.0003	0.22 ± 0.02	0.5 ± 0.1	0.57 ± 0.07	0.004 ± 0.006	0.0005